



## Topical co-delivery of methotrexate and etanercept using lipid nanoparticles: A targeted approach for psoriasis management



Mara Ferreira<sup>a</sup>, Luísa Barreiros<sup>a</sup>, Marcela A. Segundo<sup>a</sup>, Tiago Torres<sup>b</sup>, Manuela Selores<sup>b</sup>, Sofia A. Costa Lima<sup>a,\*</sup>, Salette Reis<sup>a</sup>

<sup>a</sup> UCIBIO-REQUIMTE, Departamento de Ciências Químicas, Faculdade de Farmácia, Universidade do Porto, Rua de Jorge Viterbo Ferreira, 228, 4050-313 Porto, Portugal

<sup>b</sup> Serviço de Dermatologia do Centro Hospitalar e Universitário do Porto, Instituto de Ciências Biomédicas Abel Salazar, Universidade do Porto, Rua D. Manuel II, s/n, 4099-001 Porto, Portugal

### ARTICLE INFO

#### Article history:

Received 13 April 2017

Received in revised form 12 July 2017

Accepted 27 July 2017

Available online 29 July 2017

#### Keywords:

Carbopol hydrogel

Etanercept

HaCaT keratinocytes

Human skin permeation

Methotrexate

Psoriatic skin

Solid lipid nanoparticles

### ABSTRACT

Methotrexate is indicated in psoriasis systemic therapy and its topical administration may be an option to overcome several side effects. A targeted delivery may be achieved through etanercept. Thus, a combination targeted therapy using methotrexate and etanercept could bring new perspectives for psoriasis patients. This work intended to develop and characterize co-delivery of methotrexate and etanercept using lipid nanoparticles, mediated by a carbopol hydrogel and to evaluate their potential for delivering the drug into the skin with reduced transdermal permeation. The nanoparticles were physico-chemically characterized. *In vitro* methotrexate release from solid lipid nanoparticles revealed a sustained release for 8 h. The solid lipid nanoparticles were non-toxic towards human keratinocytes and fibroblasts. Permeation studies using pig ear as model revealed enhanced skin deposition of the applied methotrexate when incorporated within solid lipid nanoparticles in relation to free drug. Therapeutic amounts of methotrexate were delivered to psoriatic human skin after application of solid lipid nanoparticles, with reduced transdermal permeation.

© 2017 Elsevier B.V. All rights reserved.

### 1. Introduction

Psoriasis is a common, chronic, immune-mediated disease, affecting over 125 million people around the world, associated with significant negative impact on the patient's quality of life [1]. Histologically, psoriatic lesions are characterized by epidermal acanthosis, due to keratinocyte proliferation and altered differentiation, neutrophil migration, angiogenesis and cutaneous infiltration of inflammatory cells on the dermis and epidermis [2]. Approximately 80% of those affected with psoriasis have mild-to-moderate forms and are usually treated with topical therapy, whereas phototherapy and systemic therapies are used for those with severe disease.

Although in the past years several systemic therapies have been developed and approved for the treatment of psoriasis, topical agents have been neglected over the last 20 years. Nevertheless, topical administration is the preferable route for skin-related diseases whose triggers are underneath the skin as it results in a more efficient action, reduces drug systemic toxic effects and has higher

patient compliance [3]. In fact, topical corticosteroids and vitamin D3 analogs are still the gold standard of therapy for mild-to-moderate. However, these therapies may be associated with lower efficacy, poor tolerability or important cutaneous side effects due to prolonged use. Topical agents have the advantage of exert local effect without exposing the patient to systemic exposure. Thus, there is the need to develop new and more effective topical agents in the short and long term, without the side effects of current therapies [4].

In psoriasis the inflammatory process is strongly related to an excessive immune response, thus immunosuppressants, such as methotrexate (MTX), have shown good efficacy. Orally-administrated MTX has a relative lower bioavailability to the one obtained by parenteral administration, due to the variable intestinal absorption as well as first-pass metabolism in the liver [5]. There is a large number of adverse effects associated to systemic administration of MTX [6], where liver toxicity can be highlighted as the most important adverse effect for long-term treatment in psoriasis patients. Nevertheless, MTX remains the gold standard of systemic treatment in the context of moderate to severe plaque psoriasis, namely when the disease is unresponsive to topical or phototherapy or when other possible therapeutic options are contraindicated for certain patients.

\* Corresponding author.

E-mail address: [slima@ff.up.pt](mailto:slima@ff.up.pt) (S.A. Costa Lima).

Biological therapeutic strategies target the immune system, thereby avoiding an increased number of adverse effects [7]. Etanercept is one of the FDA-approved existing TNF- $\alpha$  inhibitor molecules for moderate to severe plaque psoriasis treatment [8,9]. It binds to soluble TNF- $\alpha$  and, as a result, lowers its free concentration in the serum and prevents activation of inflammatory cascades. Even though prescription of biological agents, as etanercept, is associated with high costs [10], their elevated efficacy might reflect itself in the decrease of expenses related with the need or the length of hospitalization associated with other therapies.

Combination therapy is a very common therapeutic strategy in the management and treatment of mild, moderate and severe psoriasis. Indeed, this allows the creation of multiple therapeutic approaches that not only have the objective of decreasing the amount of adverse side effects, but also increase the efficacy of current treatments, and treat even the most serious refractory cases of psoriasis [11]. In fact, improved clinical efficacy and better skin tolerability of betamethasone dipropionate and calcipotriol combination, as Daivobet<sup>TM</sup>, has been well documented [12–14]. In view of the individual contribution of MTX and of etanercept in the treatment of psoriasis it is possible to envisage a combination therapy into a targeted approach based on the immunopathophysiology of this illness [15].

Stratum corneum (SC) act as a major obstacle for topical therapy [3,16]. To overcome these limitations and drawbacks, nanomedicine approaches involving nanocarriers and hydrogels could be a remarkable option. In particular, solid lipid nanoparticles (SLNs) present many advantages for targeted topical administration of drugs. Both the lipids and surfactants employed in the production of SLNs are generally regarded as safe (GRAS) substances and are low-priced excipients; SLNs are usually stable, protect drug from degradation and allow a prolonged drug release; and their production can be easily scaled-up [17]. In the scope of topical administration, SLNs possess features that render them ideal, such as the possibility for small particle size, with occlusive ability, thus increasing skin moisture and hydration and, consequently, drug permeation [3]. Therefore, SLNs seem to be an interesting approach for effective delivery to basal epidermis, which is the site of action for psoriasis.

The objective of the present study was to investigate SLNs as delivery systems for MTX and etanercept combination therapy and to develop a simple and unique hydrophilic formulation for topical psoriasis treatment. MTX was loaded into SLNs and etanercept-conjugated SLNs by hot ultrasonication method and characterized for particles size, polydispersity, surface potential, protein coupling efficiency, drug entrapment efficiency, biocompatibility and drug *in vitro* release. Both types of SLNs were further incorporated into a carbopol hydrogel for ease topical application and the rheological properties were assessed. The *in vitro* skin permeation was evaluated in pig ear skin as a model, and human biopsies from healthy and psoriatic skin to determine the potential skin deposition and permeation.

## 2. Experimental section

### 2.1. Materials

The methotrexate was kindly provided by Excella (Feucht, Germany) and the etanercept was a courtesy from FairJourney Biologics (Porto, Portugal). Cetyl palmitate was a kind gift by Gatefossé (France). All other chemicals and solvents were of analytical grade acquired from Sigma-Aldrich (St Louis, USA) unless stated otherwise. Aqueous solutions were prepared with double-deionized water (Arium Pro, Sartorius AG, Göttingen, Germany), which possesses conductivity values lower than 0.1  $\mu\text{S cm}^{-1}$ . Fetal bovine

serum (FBS), penicillin-streptomycin antibiotics mixture and Dulbecco's Modified Eagle's Medium (DMEM) were purchased from Gibco<sup>®</sup> (Invitrogen Corporation, UK). L929 mouse fibroblast cell line was obtained from ATCC-LGC Standards (Barcelona, Spain) and HaCaT keratinocyte cell line was obtained from CLS (Eppelheim, Germany).

### 2.2. Methods

#### 2.2.1. Production of solid lipid nanoparticles containing MTX

SLNs were produced using hot ultrasonication method [18]. Briefly, melted cetyl palmitate (150 mg) was dispersed in 7 mL pre-heated water containing 47 mg of polysorbate 80, in a water bath set to 10° above the melting point of the solid lipid. Methotrexate (10% (w/w)) was incorporated upon addition to the lipid phase. Then, the coarse emulsion was sonicated using a probe sonicator (VCX130, Sonics & Materials, 115 Newtown, CT, USA) with amplitude frequency of 70% during 10 min, in order to obtain a nanoemulsion (Fig. S1). The formulations were left to cool down and stored at room temperature until further use.

#### 2.2.2. Functionalization of lipid nanoparticles for psoriasis targeting

Etanercept was selected as a targeting protein due to its biological effect in the therapy of psoriasis. For the functionalization of SLNs with the monoclonal antibody etanercept, 5 mg of DSPE-PEG-NH<sub>2</sub> were added to the lipid phase during the production process. Upon ultrasonication the DSPE-PEG-NH<sub>2</sub> containing SLNs were incubated with 100  $\mu\text{g}$  of 1-ethyl-3-(3 dimethylaminopropyl) carbodiimide (EDC) in 20 mL of phosphate buffered saline (PBS), mixed and incubate for 30 min at 4 °C (Fig. S1). Then, 10  $\mu\text{L}$  of etanercept were added and activated by the EDC in solution to allow the carbodiimide reaction with the SLNs. After overnight dialysis against phosphate buffered saline using a specific membrane (molecular weight cut off 6000–8,000 Da, CelluSep1 T2; Membrane Filtration Products Inc., Frilabo, Portugal) to remove remaining reagents and uncoupled etanercept, functionalized SLNs were placed at 4 °C until further use [19]. The protein coupling efficiency was determined in the previously dialyzed sample using a BioRad protein assay (BioRad Laboratories, Inc., Amadora, Portugal) and quantification at 750 nm in a BioTek (Sinergy HT, BioTek Instruments Inc., Winooski, VT, USA) microplate reader, as recommended by the manufacturer.

#### 2.2.3. Physicochemical characterization

The particle size, polydispersity index (PDI) and zeta potential of the nanoformulations were analyzed using a ZetaPALS zeta potential analyzer (Brookhaven Instruments Corporation, Holtsville, NY, USA). Particle size and PDI were evaluated by dynamic light scattering (DLS) and zeta potential was determined by electrophoretic light scattering (ELS). All samples were diluted (1:400) with double distilled water and analyses were carried out of 25 °C with a fixed light incidence angle of 90 °C. For each sample, the corresponding mean standard deviation values were obtained from six runs of ten cycles and calculated by the multimodal analysis. The determination of MTX entrapment efficiency followed previous reports [18,20]. Briefly, standard MTX solutions were prepared at 0.75, 1.5, 3, 6, 12.5 and 25  $\mu\text{g mL}^{-1}$  in mobile phase and in permeation buffer enriched upon pig skin contact for defined times (0, 1, 3, 5 and 8 h). For the HPLC analysis a Chromolith 4.6-mm reversed-phase monolithic column (Merck, Darmstadt, Germany) was used as a stationary phase. The HPLC system included MD-2015 multi-wavelength detector (Jasco, Easton, MD, USA) programmed for peak detection at 303 nm, a high-pressure pump (PU-2089), an autosampler (AS-2057) and a controller (LC-Net II/ADC) mastered by ChromNAV software. For the morphological (surface structure and shape) characterization the SLNs and functionalized SLNs were

analyzed by TEM (TEM Jeol JEM-1400, Tokyo, Japan). TEM images were acquired after sample staining with uranyl acetate for 30 s on the surface of carbon coated copper grid and under accelerating voltage of 60 kV.

#### 2.2.4. In vitro drug release

The MTX *in vitro* release from the lipid nanoparticles was investigated using a dialysis technique under sink condition. PBS pH 7.4 or acetate buffer at pH 5.0 were used as dissolution medium (maintained at  $37 \pm 0.5^\circ\text{C}$  and  $32 \pm 0.5^\circ\text{C}$ , to mimic physiological and skin temperature, respectively), which is equivalent to the pH of the skin and inflamed skin respectively. MTX-loaded SLNs dispersion (1.5 mL) containing 250  $\mu\text{g}$  of MTX was first poured into the dialysis bag (molecular weight cut off 6000–8000 Da, CelluSep1 T2; Membrane Filtration Products Inc., Frilabo, Portugal) with the two ends fixed by thread and placed into the preheated dissolution media. The suspension was stirred at defined temperatures, using a heating and magnetic stirring plate (IKAMAG1, Staufen, Germany) at 350 rpm. One mL of the sample was withdrawn at fixed time intervals and the same volume of fresh medium was added accordingly. The drug content was determined spectrophotometrically (Jasco V-660 spectrophotometer, Easton, MD, USA), and several mathematical models for evaluation of drug release kinetics (zero order, first order, Higuchi, Peppas-Korsmeyer and Hixon-Crowell) were fitted to the experimental data [21]. Regression coefficient ( $r^2$ ) was calculated to determine the best-fit model.

#### 2.2.5. Hydrogel-enriched SLNs

Hydrogels were produced using Carbopol<sup>®</sup> 934: a certain amount of polymer (0.5, 1, 1.5 or 2% (w/w)) was hydrated in 25 mL of double-distilled water using a stirrer at a speed of 150 rpm overnight. NaOH solution (10%) was added dropwise to neutralize the solution until it turned into a transparent gel, conferring a pH value within the range to 5.5–7.4, similar to the dermal conditions. The pH was confirmed with universal pH strips. The gel with the concentration of carbopol that had the best consistency considering its spreadability and rheological behavior was selected for the incorporation of the empty or drug-loaded lipid nanoparticles.

#### 2.2.6. Cell culture studies: viability assessment

Fibroblasts (L929 cell line) and keratinocytes (HaCaT cell line) were cultivated in DMEM medium supplemented with 2% glutamine (v/v), 10% fetal bovine serum (v/v), and 1% streptomycin/penicillin. Cells were maintained in a humidified chamber at  $37^\circ\text{C}$  and 5%  $\text{CO}_2$ , and when reaching 80% confluence they were detached using trypsin 0.25% (w/w). L929 and HaCaT cells were cultured in 96-well plates at  $5 \times 10^4$  cell  $\text{mL}^{-1}$  density and after 20 h incubated with the lipid nanoparticles at different concentrations (ranging from 0.1–100  $\mu\text{g mL}^{-1}$  in MTX). Empty SLNs were added at equivalent lipid concentration to the MTX-loaded SLNs (15–250  $\mu\text{g mL}^{-1}$ ) in order to expose all cells to the same amount of SLNs. Upon 24 or 48 h of incubation, the culture medium was removed and replaced by 100  $\mu\text{L}$  of MTT at 0.5  $\text{mg mL}^{-1}$  in fresh culture medium. After 3 h at  $37^\circ\text{C}$  the formazan crystals were solubilized using 100  $\mu\text{L}$  of DMSO and absorbance (590 nm, 630 nm) was read using a Synergy<sup>™</sup> HT Multi-mode microplate reader.

#### 2.2.7. Ex vivo pig ear skin permeation studies

To assess MTX permeation through the skin, pig ear skin was mounted on standard Franz diffusion cells (9 mm unjacketed Franz diffusion cell with 5 mL acceptor volume, o-ring joint, clear 216 glass, clamp and stir-bar; PermeGear, Inc., Hellertown, PA, USA). For the skin permeation of free MTX, and MTX-loaded in SLNs or in SLNs-etanercept, an equivalent amount of 250  $\mu\text{g}$  in drug was added to the donor medium. The receptor medium (5 mL) was composed by PBS pH 7.4 with 10% DMSO, added to maintain

sink conditions. The stirring rate and temperature of receptor were respectively kept at 600 rpm and  $32.0 \pm 0.5^\circ\text{C}$ , and at appropriate intervals, 500  $\mu\text{L}$  aliquots of the acceptor medium were withdrawn and immediately replaced with equal volumes of fresh buffer. The samples were kept at  $-20^\circ\text{C}$  until further HPLC quantification.

#### 2.2.8. Ex vivo human skin permeation studies

Healthy and psoriatic human skin biopsies samples were collected from three donors from the Dermatology Service at Centro Hospitalar do Porto (Porto, Portugal). The study was approved by the Committee for Ethics in Research (Ref: 2015.090 (084 DEF1/079-CES)). Hypodermis and fatty tissue were removed and discs with a thickness of ca. 0.8 mm were used for the permeation studies. One hundred  $\mu\text{g}$  of drug as free solution and incorporated in lipid nanoparticles (SLNs and SLNs-etanercept) were added to the donor compartment. The receptor compartment (PBS pH 7.4 with 10% (v/v) DMSO) was agitated at room temperature during 1, 4, 6 and 8 h. At each time point, the donor and receptor compartments were withdrawn to quantify permeation of MTX. Samples were centrifuged 10,000 rpm, 15 min prior HPLC analysis, as previously described. The skin samples were carefully washed for 15 s under running water to remove the residual formulation from the stratum corneum surface and then cut into small pieces. The deposited MTX was extracted by soaking the skin in 2 mL of acetonitrile, for 4 h with continuous stirring at room temperature.

#### 2.2.9. Statistical analysis

Data is expressed as the mean  $\pm$  standard deviation, for a minimum of three independent experiments. Statistical comparisons of the means were performed using one-way analysis of variance or Student's *t*-test with Welch's correction, Mean  $\pm$  SD ( $n = 3$ ); \* $P < 0.05$ , \*\* $P < 0.01$  obtained with one-way ANOVA analysis with GraphPad Prism 6 software (La Jolla, California, USA). The differences were considered to be significant when the *P*-value was  $< 0.05$ .

### 3. Results and discussion

#### 3.1. Characterization of SLNs for co-delivery of MTX and etanercept

Cetyl palmitate SLNs loaded with MTX were produced by hot ultrasonication technique, with polysorbate 80 as surfactant. The incorporation of an amine-terminated DSPE allows conjugation with antibodies, such as etanercept, on the surface through a covalent carboxyl-amine linkage. Co-delivery of etanercept through functionalized SLNs will also allow a targeted delivery of nanoparticles to the immune system involved in the psoriasis pathology [15].

The dynamic laser scattering data demonstrates that the average diameter of SLNs-etanercept-MTX is  $356 \pm 2$  nm which was significantly larger than SLNs-MTX ( $292 \pm 4$  nm). Etanercept conjugation also increased significantly the average size of SLNs (Table 1).

MTX incorporation did not affect the average size of SLNs or SLNs-etanercept. The SLNs had a PDI in the range of 0.187 (SLNs) to 0.214 (SLNs-etanercept-MTX) and maintained colloidal stability up to 72 h under physiological pH. The PDI values suggest that the lipid nanoparticles suspension is homogenous with low tendency for aggregation [22]. The determination of zeta potential values on the SLNs and conjugated-SLNs were carried out to achieve more information on the nanoparticles stability. Data obtained evidenced zeta potential values around  $-30$  mV (from  $-31$  mV to  $-27$  mV), ascertain for the nanoparticles stability and revealing that they do not tend to form aggregates [23]. MTX incorporation and the etanercept-conjugation did not have significant interference in the zeta potential values and consequently in the stability of the formulations (Table 1). The entrapment efficiency of methotrexate was

**Table 1**  
Physicochemical characterization of lipid nanoparticles for co-delivery of MTX and etanercept.

	Size (nm)	PDI	$\zeta$ -potential (mV)	EE (%)
SLNs	298 ± 5	0.187 ± 0.009	-30 ± 2	
SLNs-MTX	292 ± 4	0.191 ± 0.011	-28 ± 3	85 ± 1
SLNs-etanercept	349 ± 3*	0.212 ± 0.008	-31 ± 2	
SLNs-etanercept-MTX	356 ± 2*	0.214 ± 0.012	-27 ± 4	88 ± 2

Mean ± SD (n = 3); \*  $P < 0.5$  obtained with one-way ANOVA analysis applying Dunett's test for comparison among lipid nanoparticles and conjugated lipid nanoparticles.

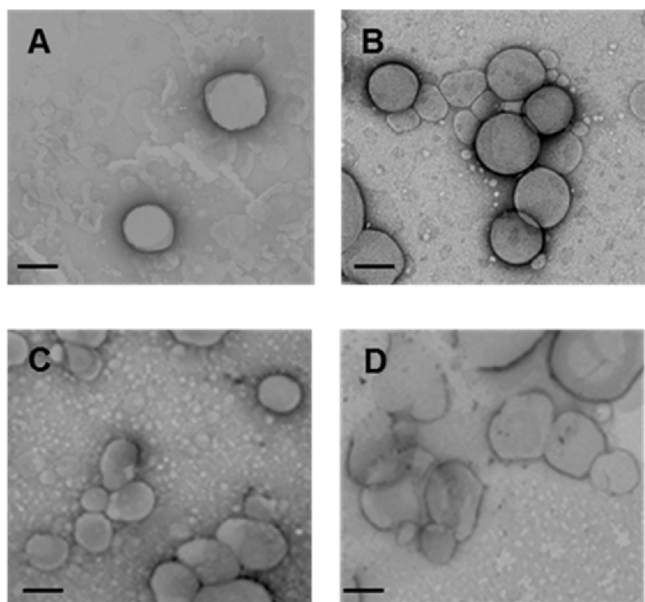


**Fig. 1.** Characterization of SLNs for co-delivery of MTX and etanercept. Transmission electron microscopy of SLNs (A), SLNs-etanercept (B), SLNs-MTX (C) and SLNs-etanercept-MTX; the scale is of 200 nm.

about 85% for SLNs and 88% for SLNs-etanercept, which indicate that functionalization process did not affect the drug incorporation.

The larger size of etanercept-conjugated lipid nanoparticles was also verified by transmission electron microscopy (Fig. 1). These images confirm the nanometer range of the SLNs as determined by DLS (Table 1) and also show the increase in size observed with the addition of MTX and etanercept (Fig. 1B/C vs Fig. 1D). The data was confirmed in a minimum of three batches and the successful antibody conjugation to SLNs was shown by protein quantification. SLNs-etanercept and SLNs-etanercept-MTX presented higher protein levels when compared to SLNs and SLNs-MTX, due to the antibody conjugation (Fig. S2).

Storage stability at 25 °C was analyzed by changes in particle size, PDI, zeta potential and drug content of lipid nanoparticles as compared with freshly prepared formulations. No visual changes or aggregation were observed. Data gathered for 8 weeks is represented on Fig. S2 and reveals no statistically significant alterations in the assessed parameters. Moreover, drug content remained constant at levels around 15 mg of MTX, equivalent to 85% (w/w) drug content, in the lipid nanoparticles suspension.

### 3.2. In vitro methotrexate release studies

A relevant issue for dermatological applications is the drug release kinetics [24]. Hence, *in vitro* release profile of MTX from SLNs and SLNs-etanercept was evaluated by drug diffusion through dialysis membrane for 8 h in different pH and temperature conditions simulating the physiological (pH 7.4, 37 °C) and the skin (pH 5.0, 32 °C) environments. Data shown in Fig. 2 exhibits the obtained profiles of MTX released from the lipid nanoparticles as a function

of time. The cumulative MTX release from SLNs was similar under skin environment and physiological conditions, reaching ca. 50% release in 8 h period. A biphasic pattern was observed for all the lipid nanoparticles studied, exhibiting an initial fast release of ca. 15% in the initial 30 min and then a slow phase reaching values of 51 ± 5% and 44 ± 3%, for SLNs and SLNs-etanercept, respectively after 8 h under skin-simulated environmental. Similar profile was observed at physiological-simulated conditions, with SLNs releasing about 44 ± 4% and SLNs-etanercept 52 ± 4% of MTX in 8 h. The co-delivery of both antipsoriatic agents by SLNs did not influence the release of MTX under the studied conditions. In dermatological application, an initial fast release phase can enhance drug penetration while a sustained release allows the presence of drug for a longer period of time. A fast drug release with zero order kinetics was observed for free MTX, under both studied conditions (Fig. 2).

For both types of lipid nanoparticles containing MTX, the release kinetics followed the Peppas-Korsmeyer pattern ( $r^2$ : 0.9205 and 0.9345, for physiological, and 0.9890 and 0.9912 for skin simulated environments). The Peppas-Korsmeyer model describes a diffusion-controlled drug release profile for lipid nanoparticles [25–27]. Moreover, Table S1 shows that  $n$  values, release component indicative of drug release mechanism, found for each condition are around 0.5, suggesting that quasi Fickian diffusion occurs by the usual molecular diffusion of the drug [28]. Similar results attributing diffusion-controlled release of MTX from nanostructured lipid carriers were obtained by Ferreira et al. [29], but with higher  $n$  values defining a non Fickian diffusion, as a combination of both diffusion and erosion controlled rate release probably related to the different structure, lipid and surfactant composition of the nanoparticles.

### 3.3. Influence of lipid nanoparticles on cell viability

Biocompatibility of SLNs and conjugated SLNs were tested in the presence of human keratinocytes (HaCaT cell line) and L929 fibroblasts, as recommended for the safety assessment (ISO 10993-5, 2009). Cells do not display changes after treatment with empty SLNs when compared to the control group (Fig. S3). Human HaCaT keratinocytes viability was affected by free MTX, as cellular viability decreased to 75% with 250  $\mu\text{g mL}^{-1}$  of drug. The presence of MTX on the SLNs reduced to 80% the cell viability, at a 250  $\mu\text{g mL}^{-1}$  drug concentration. Etanercept conjugation did not influence the cells viability in relation to non-treated cells. Cell viability above 80% indicates that the treatment is not toxic. The biocompatibility data indicate that the lipid nanoparticles have potential for delivery of MTX, as concentrations of drug close to 125  $\mu\text{g mL}^{-1}$  of MTX do not affect cell viability, confirming the safety of the delivery system.

### 3.4. Rheological properties of hydrogel-enriched nanoparticles

The effect of different amounts (0.5; 1; 1.5 and 2% (w/w)) of Carbopol® 934 to produce 25 g of hydrogel was screened. For lipid nanoparticles incorporation the 1.5% (w/w) carbopol hydrogel was selected due to its better spreadability properties as observed in Fig. S4 with a lower value of shear stress when compared to 2% (w/w) carbopol hydrogel.

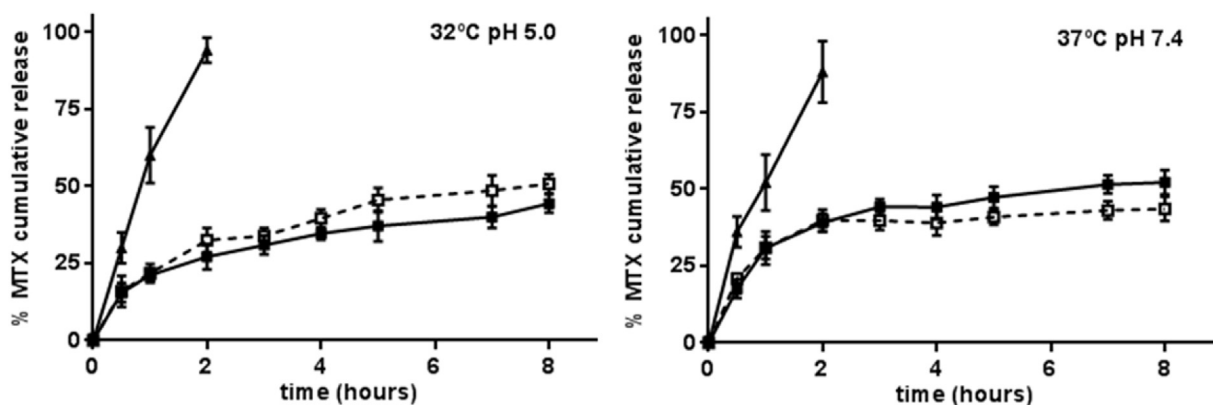


**Fig. 2.** MTX *in vitro* release. Cumulative drug release from free MTX (closed triangles) and MTX-loaded in SLNs (open squares) and SLNs-etanercept (closed squares) under skin (32 °C, pH 5) and physiologic (37 °C, pH 7.4) simulated environments for 8 h. Data represent mean  $\pm$  SD (n = 3).

### 3.4.1. Incorporation of SLN co-delivering MTX and etanercept in carbopol hydrogel

The 1.5% (w/w) carbopol hydrogel was enriched with 6 mg of free MTX and the rheological properties were evaluated. It is possible to observe that the hydrogel enriched with MTX did not retained thixotropy, as flow curves are totally overlapped which indicates that MTX completely changes the hydrogel structure (Fig. S5). This result hampers the use of carbopol 1.5% (w/w) as carrier of free MTX in topical applications because it changes the thixotropic properties of the hydrogel base [30]. Empty SLNs and MTX-loaded SLNs and conjugated-SLNs were incorporated into the 1.5% (w/w) carbopol hydrogel, resulting in nanoparticles-enriched hydrogels. Rheological assessment revealed that the flow curve do not overlap (Fig. S5B–D), thus the hydrogels maintain thixotropy. As observed previously, the presence of MTX lowers the hydrogel thixotropy and spreadability, translating a decreased ability to return of their initial properties, after application of shear stress. It is possible that conjugated SLNs increase the viscosity of nanoparticles due to the aggregation of protein contributing to the observed outcome [31].

### 3.4.2. Storage stability of hydrogel enriched nanoparticles

Storage stability of 1.5% (w/w) carbopol hydrogel and hydrogel enriched nanoparticles was assessed after 2 weeks of preparation. All of hydrogels appeared transparent, glossy and uniform within this period of time. Furthermore, their rheological parameters were measured in order to investigate any changes in the pseudoplastic properties and thixotropy and no differences were observed after 2 weeks storage at room temperature. Moreover, for hydrogel enriched nanoparticles (protein-conjugated or not) similar pseudoplastic behavior was observed as upon preparation, thus all formulations presented thixotropy. However, a decrease in shear stress value was detected along time, which meant a small shear in the gel to cause the gel to flow. This behavior could be explained by the existence of certain internal structures that change with flowing; as particles aggregates, formed by hydrogen bonds or van der Waals interactions, that could break and promote a small decrease in its consistency [32,33]. For these reasons it seems that although the formulations presented a small decrease in shear stress they remained a good option for topical application, due to pseudoplastic and thixotropy properties.

## 3.5. Skin permeation studies

### 3.5.1. Pig ear permeation assay

Skin permeation study is a crucial step in the characterization of formulations for topical administration [34]. The skin penetration assessment of MTX and etanercept co-delivered through SLNs was

conducted using Franz diffusion cells. Pig ear skin was chosen as a model barrier, due to its similarity, in morphology and function, to its human counterpart. As can be seen from Fig. 3A, MTX delivered from the SLNs permeated through the pig ear skin at a higher extent as compared to free MTX. Upon 8 h,  $1.7 \pm 0.1\%$ ,  $3.1 \pm 0.1\%$  and  $3.8 \pm 0.2\%$  of MTX permeated the skin delivery as free, loaded in protein-conjugated SLNs and loaded in SLNs, respectively. As it has been described, lipid nanoparticles improve drug skin permeation in relation to free drug [35,36]. Hence, lipid nanoparticles play an important role in controlling the MTX delivery through the skin. Protein-conjugated SLNs permeated the skin, according to MTX quantification and DLS measurements, but at non-detectable protein levels (Fig. 3B). Protein conjugation to SLNs could act as a double barrier for the drug diffusion process mediated by the structural integrity conferred by protein coupling, thus decreasing drug penetration profile [19].

At the end of the permeation assay, the formulation that remained on top of the skin was recovered and the skin washed twice for quantification of non-permeated drug. About 38% of the initial added amount of MTX did not penetrate or permeate the skin, while 22% and 15% were found for the conjugated-SLNs and SLNs formulations, respectively. When incorporated in the lipid nanoparticles, MTX accumulated in skin in significantly higher amounts when compared to its free solution. However, only few studies were performed using porcine skin for topical assessment of MTX combination therapy. Nanostructured lipid carriers of Pre-circol ATO 5 and squalene used for co-delivery of calcipotriol and methotrexate were described by Lin et al., and exhibited permeation rates around  $1 \mu\text{g}/\text{cm}^2/\text{h}$  for MTX [37].

Gathering the permeation assay information, it can be taken that a low amount of MTX and non-detectable amount of etanercept was permeated through pig ear skin up to 8 h (Fig. 3) suggesting that SLNs were mainly confined to the epidermal, dermal and SC of the skin. Hence, negligible drug permeation will further minimize the systemic side effects due to insignificant absorption into systemic circulation [38].

Skin permeation studies were also performed for the 1.5% (w/w) carbopol hydrogel-enriched with lipid nanoparticles. The drug flux rate was determined after 8 h of skin permeation and compared with the lipid nanoparticles in suspension (Table S2). Reflecting the data shown on Fig. 3A, the incorporation of MTX in lipid nanoparticles resulted in an increase of the drug flux rate through the skin of 1.7-fold and 2.3-fold for protein-conjugated SLNs and SLNs, respectively. Free MTX incorporated in the carbopol hydrogel permeated 1.7-fold more in relation to drug in solution. This data correlates with the rheological properties described previously, and may account for the changes in the hydrogel structure induced by

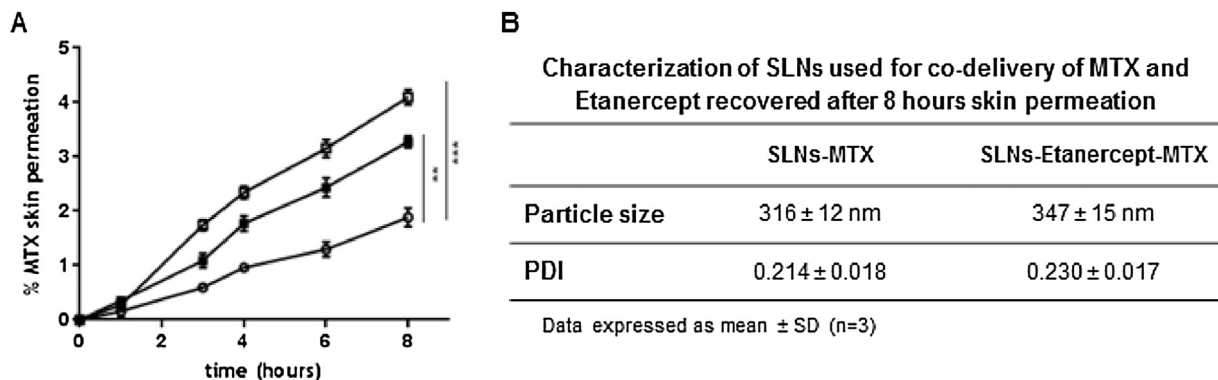


**Fig. 3.** Characterization of the MTX permeation through pig ear skin. (A) Drug permeation over 8 h assay as free MTX (open circles), SLNs-etanercept-MTX (black square) and SLNs-MTX (black square), data represent mean ± SD (n=4), \*\*  $P < 0.01$  and \*\*\*  $P < 0.001$  in relation to free MTX. (B) Characterization of SLNs collected on the receptor compartment of the Franz cell diffusion system after 8 h by DLS assessment.

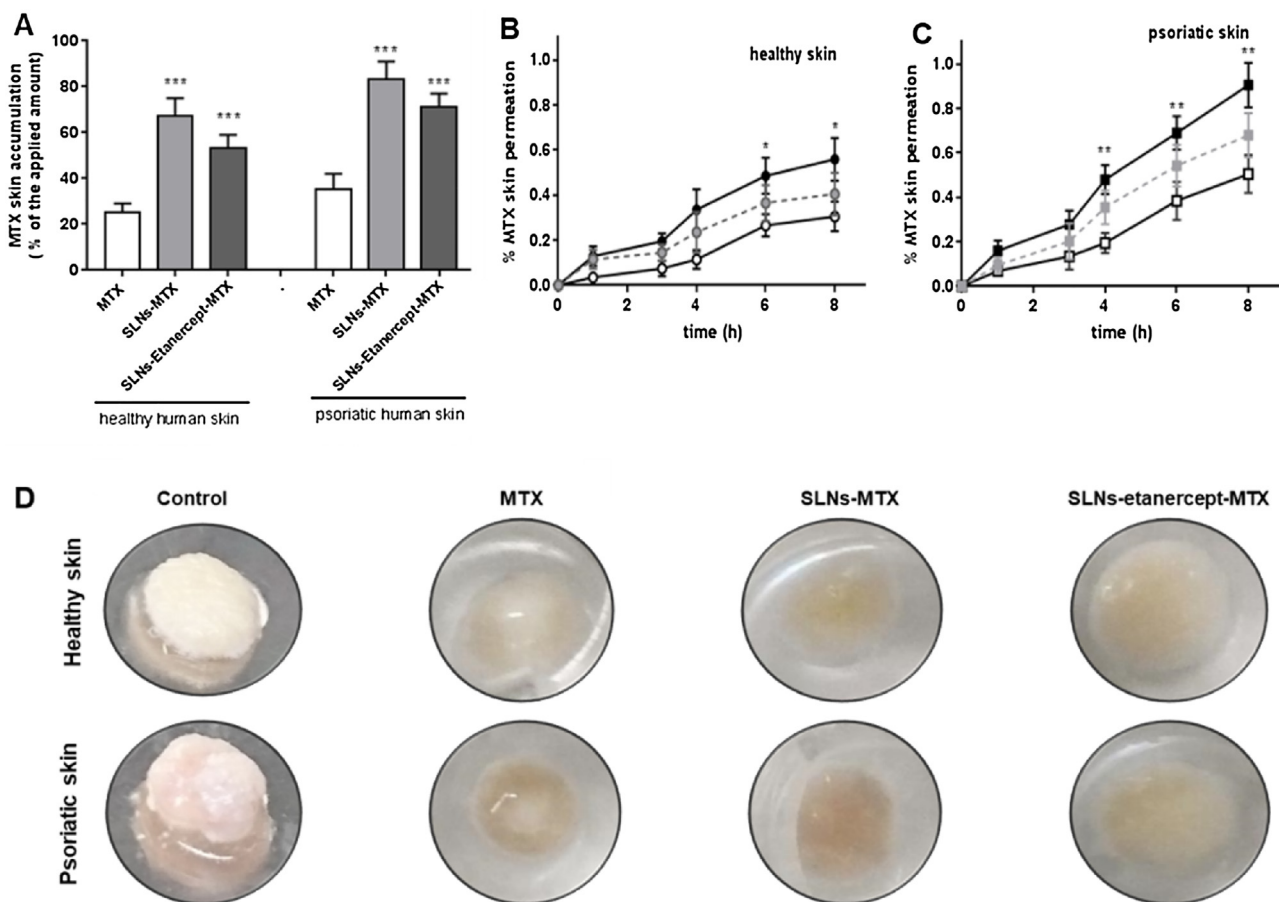


**Fig. 4.** MTX skin deposition in human healthy and psoriatic skin. (A) Accumulation of MTX after 8 h permeation in healthy and psoriatic skin, after application of free MTX and MTX-loaded in SLNs and in SLNs-etanercept. (B) Amount of MTX that permeated the human skin as a function of time up to 8 h. Data expressed as mean ± SD, \*\*\*  $P < 0.01$ , \*\*\*\*  $P < 0.001$ . (D) Visual appearance of the human skin samples prior (control) and after 8 h in contact with the formulations of free MTX and MTX-loaded in SLNs and in SLNs-etanercept.

the MTX with consequent loss of consistency that could facilitate skin drug permeation.

For the formulations of carbopol hydrogel enriched with lipid nanoparticles (SLNs-etanercept and SLNs) the flux rate value were  $0.75 \pm 0.08$  and  $1.07 \pm 0.11 \mu\text{g cm}^{-2} \text{h}^{-1}$ , respectively, corresponding to a 35–39% decrease in comparison to MTX loaded in SLNs and etanercept-conjugated SLNs. SLNs enriched hydrogels released drug slower when compared with SLNs dispersions, accounted for the time drug takes to diffuse through the gel. The slower release of drug from hydrogels-enriched SLNs maintained the drug con-

centration for longer period of time in the skin, as observed by others [39]. When lipid nanoparticles are embedded in the carbopol hydrogel a smaller amount of MTX permeates, perhaps related to the mucoadhesive properties of the hydrogel that enhance the retention time of MTX. Similarly, Gonzalez-Mira and co-authors observed that the delivery of flurbiprofen in lipid nanoparticles-based hydrogels formulations increased the drug residence time in the corneal tissue in relation to the lipid nanoparticles dispersions [40].

### 3.5.2. Human skin permeation: healthy versus psoriatic

The promising results of skin permeation using pig ear skin persuaded to study the permeation of MTX-loaded in lipid nanoparticles and free MTX formulation using human biopsies representing healthy and psoriatic skin. The MTX accumulated within the skin at a higher extent when incorporated in the lipid nanoparticles, in relation to MTX solution (Fig. 4A). About 70–85% of the applied dose was deposited within the skin layer in the form of SLNs-MTX, for healthy and psoriatic skin, respectively (Fig. 4A). Etnarcept conjugated SLNs retained MTX in the skin around to 60% in healthy skin and 75% in diseased skin. Thus dermal bioavailability of MTX was increased significantly for SLNs dispersion in both healthy and psoriatic skin. The latter damaged skin facilitated the penetration of drug to the skin layers. MTX skin deposition after 8 h from SLNs formulations reached  $70 \pm 2 \mu\text{g}$  and  $84 \pm 3 \mu\text{g}$  for healthy and psoriatic skin from a dose of  $100 \mu\text{g}$ , respectively (Fig. 4A). As the skin barrier is compromised, due to pathological processes, SLNs penetration in psoriatic skin might be considerably facilitated. Indeed, the alteration of the stratum corneum associated with inflammation and keratinocyte hyperproliferation could aid in the penetration of nanoparticles in psoriatic lesions [41]. The permeation study demonstrated identical profile as observed using pig skin, since MTX-loaded SLNs permeated 1.7-fold more than free drug after 8 h of study, in healthy skin (Fig. 4B). The assay using psoriatic skin revealed the same tendency but at a higher extent (Fig. 4C). At the end of the 8 h assay it was possible to observe differences at the applied dose, as the formulation of free MTX was clearly still on top of the skin, while SLNs-MTX and SLNs-etanercept-MTX formulations were absorbed through the skin (Fig. 4D).

## 4. Conclusions

Cetyl palmitate based SLNs efficiently incorporated and delivered MTX, a poorly water soluble drug. A combination therapy approach was implemented by etanercept conjugation to the SLNs. Lipid nanoparticles diameters, ranged from 292 nm for SLNs-MTX to 356 nm for SLNs-etanercept-MTX, and were biocompatible with human keratinocytes and fibroblasts. *In vitro* studies revealed a MTX sustained release profile under physiological and skin-mimetic environment. Lipid nanoparticles containing MTX and etanercept were further incorporated into a 1.5% (w/w) carbopol hydrogel, resulting in a transparent, glossy, uniform and thixotropic hydrogel. Rheological tests showed that all formulations are suitable for topical drug delivery.

SLNs-MTX and SLNs-etanercept-MTX formulations significantly enhanced the skin bioavailability of MTX in relation to the application of free drugs in solution, as demonstrated through the pig ear skin permeation assays. Moreover the carbopol hydrogel enriched with SLNs-MTX or SLNs-etanercept-MTX released drug slower when compared with SLNs dispersions, thus maintaining the drug concentration for longer period of time in the skin. The mucoadhesive properties of the hydrogel increased the MTX retention time within the skin which could improve drug therapeutic effect. Besides, a reduced amount (below 5%) of drug permeated the skin, limiting MTX and etanercept dispersion into systemic circulation, which is crucial when the diseased area is limited to the skin. Preliminary studies using human skin biopsies from healthy and psoriatic regions validated the observations from studies using pig ear skin as a model. The lipid nanoparticles were able to accumulate MTX within the skin layers at significant amounts in relation to free MTX, and with reduced permeation. The outcomes of this work can build a path forward for combinational drug therapy using

lipid nanoparticles and hydrogels for an effective and synergistic treatment of psoriasis.

## Acknowledgments

The authors are also grateful to Dr Rui Fernandes (Histology and Electron Microscopy Service – I3S, Universidade do Porto) for the expertise and technical assistance with TEM. This work received financial support from the European Union (FEDER funds POCI/01/0145/FEDER/007728) and National Funds (FCT/MEC, Fundação para a Ciência e Tecnologia and Ministério da Educação e Ciência) under the Partnership Agreement PT2020 UID/MULTI/04378/2013. SCL thanks Operação NORTE-01-0145-FEDER-000011 for her Investigator contract. LB thanks FCT/MEC and POPH (Programa Operacional Potencial Humano) for her Post-Doc grant (SFRH/BPD/89668/2012).

## Appendix A. Supplementary data

Supplementary data associated with this article can be found, in the online version, at <http://dx.doi.org/10.1016/j.colsurfb.2017.07.080>.

## References

- [1] W.H.O. Global report on psoriasis, 2016.
- [2] W.H. Boehncke, M.P. Schön, *Lancet* 386 (2015) 983.
- [3] M. Gupta, U. Agrawal, S.P. Vyas, *Expert Opin. Drug Deliv.* 9 (2012) 783.
- [4] A. Rafael, T. Torres, *Eur. J. Dermatol.* 26 (2016) 3.
- [5] S. Dogra, R. Mahajan, *Clin. Exp. Dermatol.* 38 (2013) 573.
- [6] S. Shen, T. O'Brien, L.M. Yap, H.M. Prince, C.J. McCormack, *Australas. J. Dermatol.* 53 (2012) 1.
- [7] I.H. Kim, C.E. West, S.G. Kwatra, S.R. Feldman, J.L. O'Neill, *Am. J. Clin. Dermatol.* 13 (2012) 365.
- [8] E. Kupetsky, A.R. Mathers, L.K. Ferris, *Cytokine* 61 (2013) 704.
- [9] T.U. Nguyen, J. Koo, *Clin. Cosmet. Investig. Dermatol.* 2 (2009) 77.
- [10] H.T. Chong, Z. Kopecki, A.J. Cowin, *BioMed Res. Int.* 2013 (2013) 168321.
- [11] S. Domm, U. Mrowietz, J. Dtsch. Dermatol. Ges. 9 (2011) 94.
- [12] L. Guenther, F. Cambazard, P. Van De Kerkhof, et al., *Br. J. Dermatol.* 147 (2002) 316.
- [13] R. Saraceno, G. Camplone, M. D'Agostino, et al., *J. Dermatol. Treat.* 25 (2014) 30.
- [14] R. Kaufmann, A. Bibby, R. Bissonnette, et al., *Dermatology* 205 (2002) 389.
- [15] G. Babino, A. Giunta, M. Ruzzetti, et al., *J. Int. Med. Res.* 44 (2016) 100.
- [16] Y.-H. Su, J.-Y. Fang, *Expert Opin. Drug Deliv.* 5 (2008) 235.
- [17] T.W. Prow, J.E. Grice, L.L. Lin, R. Faye, et al., *Adv. Drug Deliv. Rev.* 63 (2011) 470.
- [18] M.F. Pinto, C.C. Moura, C. Nunes, et al., *Int. J. Pharm.* 477 (2014) 519.
- [19] S. Shilpi, V.D. Vimal, V. Soni, *Prog. Biomater.* 4 (2015) 55.
- [20] C.C. Moura, M.A. Segundo, J.d. Neves, et al., *Int. J. Nanomed.* 9 (2014) 4911.
- [21] M. Barzegar-Jalali, K. Adibkia, H. Valizadeh, et al., *J. Pharm. Pharm. Sci.* 11 (2008) 167.
- [22] K. Mitri, R. Shegokar, S. Gohla, et al., *Int. J. Pharm.* 414 (2011) 267.
- [23] R.H. Muller, C. Jacobs, O. Kayser, *Adv. Drug Deliv. Rev.* 47 (2001) 3.
- [24] R.H. Müller, K. Mäder, S. Gohla, *Eur. J. Pharm. Biopharm.* 50 (2000).
- [25] K. Bhaskar, C. Krishna Mohan, M. Lingam, et al., *Drug Dev. Ind. Pharm.* 34 (2008) 719.
- [26] R.M. Shah, F. Malherbe, D. Eldridge, et al., *J. Colloid Interface Sci.* 428 (2014) 286.
- [27] M. Rehman, A. Madni, A. Ihsan, et al., *Int. J. Nanomed.* 10 (2015) 2805.
- [28] R.W. Korsmeyer, R. Gunny, N.A. Peppas, *Int. J. Pharm.* 15 (1983) 25.
- [29] M. Ferreira, L.L. Chaves, S.A. Lima, et al., *Int. J. Pharm.* 492 (2015) 65.
- [30] C.H. Lee, V. Moturi, Y. Lee, *J. Control. Release* 136 (2009) 88.
- [31] A.K. Jain, A. Jain, N.K. Garg, et al., *Colloids Surf. B Biointerfaces* 121 (2014) 222.
- [32] B. Jachimska, M. Wasilewska, Z. Adamczyk, *Langmuir* 24 (2008) 6866.
- [33] S.H. Song, K.M. Lee, J.B. Kang, et al., *Chem. Pharm. Bull.* 62 (2014) 793.
- [34] J.O. Morales, K. Valdés, J. Morales, et al., *Nanomedicine* 10 (2015) 253.
- [35] F.V. Tosta, L.M. Andrade, L.P. Mendes, et al., *J. Nanopart. Res.* 16 (2014) 2782.
- [36] R. Sonawane, H. Harde, M. Katariya, et al., *Expert Opin. Drug Deliv.* 11 (2014) 1833.
- [37] Y.-K. Lin, Z.-R. Huang, R.-Z. Zhuo, J.-Y. Fang, *Int. J. Nanomed.* 5 (2010) 117.
- [38] T.J. Franz, D.A. Parsell, R.M. Halualani, *Int. J. Dermatol.* 38 (1999) 628.
- [39] K. Bhaskar, J. Anbu, V. Ravichandiran, et al., *Lipids Health Dis.* 8 (2009) 6.
- [40] E. Gonzalez-Mira, S. Nikolić, A.C. Calpena, et al., *J. Pharm. Sci.* 101 (2012) 707.
- [41] P. Desai, R.R. Patilola, M.R. Singh, *Mol. Membr. Biol.* 27 (2010) 247.